REFINEMENT OF THE STOCHASTIC MODEL OF GOCE SCIENTIFIC DATA AND ITS EFFECT ON THE IN-SITU GRAVITY FIELD SOLUTION

Wolf-Dieter Schuh[1], **Jan Martin Brockmann**[1], **Boris Kargoll**[1], **Ina Krasbutter**[1], **and Roland Pail**[2]

[1]*Institute of Geodesy and Geoinformation, Department of Theoretical Geodesy, University of Bonn, 53115 Bonn, Germany, schuh@uni-bonn.de*

[2]*Institute for Astronomical and Physical Geodesy, TU München, 80290 Munich, Germany*

ABSTRACT

Within the ESA-funded project GOCE High-level Processing Facility (HPF), several methods for determining the Earth's gravity field from GOCE mission data were developed. In our approach to gravity field determination, the GOCE data are processed sequentially on a parallel computer system, iteratively via application of the method of preconditioned conjugate gradient multiple adjustment (PCGMA), and in situ via development of the functionals at the actual location and orientation of the gradiometer. This approach has been implemented within HPF as the so-called Tuning-machine in SPF6000. Its main purpose is the adjustment of the unknown stochastic model of the gradiometer observations, described by decorrelation filters and weighting factors with respect to the different observation groups (gradiometry and precise orbit information).

GOCE gradiometry (SGG) data are auto-correlated in their three components V_{xx}, V_{yy} and V_{zz} since the gradiometer measures most accurately and produces a flat error spectrum only within a certain measurement bandwidth within which it measures most accurately. From simulations the typical features and the approximate shape of the normalized spectral density function of the gradiometer data are known approximately. Based on this prior knowledge, a sequence of various AutoRegressive-Moving Average (ARMA) filters is adjusted to the actual measurement noise to remove these correlations from the observations. This adjustment is refined iteratively, as it is embedded in the estimation of the gravity field parameters and of the weighting factors. In this contribution we show the effects of various filter complexities on the final gravity field solution and the corresponding error estimates based on 71 days of real GOCE data.

Key words: GOCE; satellite gravity gradiometry; gravity field determination; gradiometer noise modeling; ARMA filters; decorrelation.

1. INTRODUCTION

As part of ESA's High HPF (SPF6000), the Tuning-machine (cf. [11], [5] and [17]) is responsible for the tuning of the stochastic model of the gravity gradients observed by GOCE's gradiometer. Based on the resulting gravity field models derived with the Tuning-machine, the final solution of the so called time-wise approach (cf. [11] and [12]) is computed at TU Graz. The Tuning-machine has the large benefit, that the computation of the full normal equation is avoided. The least squares solution is found using an iterative solver based on the method of preconditioned conjugate gradients (cf. [7], [18], [14] and [4]). Thus the computation of the gravity field from GOCE observations is very fast (2 hours on a massive parallel computer cluster for two months of data and spherical harmonic expansion up to degree and order (d/o) 240). Nevertheless the full variance/covariance matrix can only be computed via Monte-Carlo methods (cf. [1] and [2]).

We developed a special set of ARMA filters, which are well suited to model the noise of GOCE's gradiometer ([14], [15], [16] and [19]). We will show the general characteristics of the noise from the real data in Sect. 2. In Sec. 3 some filters estimated for the real data are presented, and their effect on a gradiometer only gravity field solution derived from GOCE measurements and the corresponding accuracies as part of the full variance/covariance matrix is shown. Sec. 4 shows the combination model determined within SPF6000 and the consistency of the estimated gravity field in terms of spherical harmonics. This contribution ends with a summary and an outlook.

2. CHARACTERISTICS OF THE GRADIOMETER NOISE

To get a first idea of the sophisticated noise behavior of GOCE's gradiometer, Fig. 1 shows the measured gravity gradients (in the gradiometer reference frame (GRF)) for half a day and one component (i.e. V_{zz}). Additionally, computed gravity field gradients, using the final GOCE

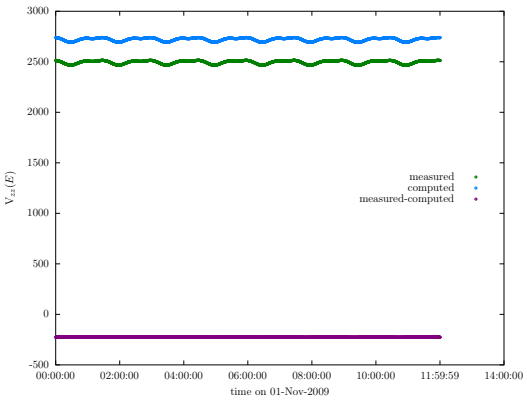

Figure 1. Measured gravity field gradients of GOCE for a half day and computed gravity field gradients from a gravity field model and the difference as a first estimation for the gradiometer noise

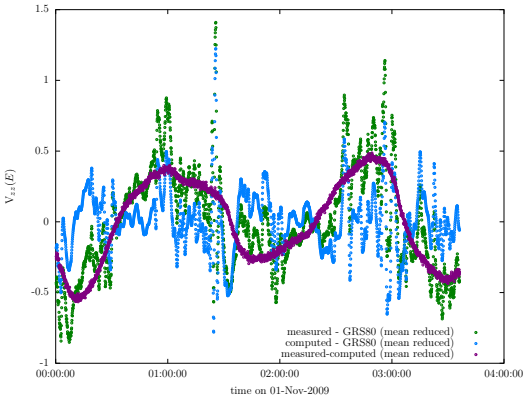

Figure 2. Reduced (mean and GRS80) measured gravity field gradients of GOCE for 3 hours and computed gravity field gradients from a gravity field model and the difference as a first estimation for the gradiometer noise

gravity field model (GO_CONS_EGM_TIM_2I, cf. [12]), are shown as timeseries. The differences of both timeseries, measured gradients minus computed gradients, are an estimation for the gradiometer noise[1]. The timeseries shown in Fig. 1 is dominated by the large bias in the measured gradients. Thus, in the displayed scale, the noise looks only like a bias. Removing the GRS80 signal from the measured and computed gradients and a mean value from the observations gives a better impression of the detailed structure of the measurement noise (cf. Fig. 2). The resulting (i.e. mean reduced) noise estimation shows now an additional drift[2] and some long wavelength oscillations, indicating the strong autocorrelations. The resulting noise is definitely non-white.

[1]Note that the three diagonal components V_{xx}, V_{yy} and V_{zz} show very similar behavior, but only the V_{zz} component is shown here.

[2]The drift is hard to recognize in this short timeseries of about 3 hours.

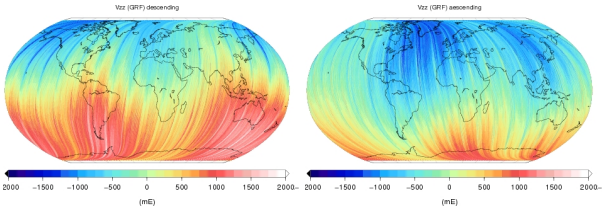

Figure 3. Mean reduced noise estimation of the gradiometer for the V_{zz} component in the spatial domain. It is dominated by a one per revolution error

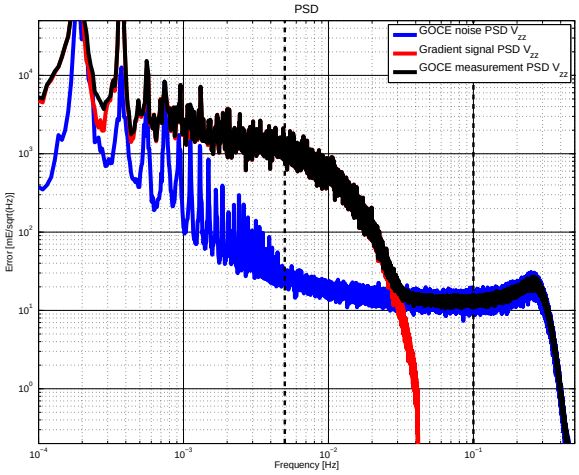

Figure 4. Error spectrum of the gradiometer noise for the V_{zz} component, the gradient signal and the measured gravity gradients

To get an idea of the spatial behavior, Fig. 3 shows the mean-reduced gradiometer noise in the GRF for ascending and descending tracks. It is dominated by a one per revolution oscillating error. These characteristics can be shown in the spectral domain of the timeseries very well. The power spectral density (i.e. the Fourier transform of the autocorrelation function) from the noise timeseries, the Earth's gravity gradient signal (computed from a set of spherical harmonics of a final GOCE solution) and the measurements themselves for the V_{zz} can be seen in Fig. 4[3].

Analyzing Fig. 4, several characteristics of the estimated gradiometer noise can be observed. Within the so-called measurement bandwidth (MBW, between 0.005 and $0.1\,Hz$), the error spectrum is more or less flat, in this bandwidth the noise is nearly white. Ranging from 0 to $0.005Hz$ the error spectrum is mainly characterized by an inverse proportional dependence (approx. $1/f$) and a large number of sharp peaks. This reflects exactly the expected behavior, which could be seen in different case studies before launch of the satellite (e.g. [16]).

[3]Note that all other components (V_{xx} and V_{yy}) have similar characteristics, but the level of the noise differs in the MBW (i.e. $\approx 8mE/\sqrt{Hz}$ for V_{xx}, $7mE/\sqrt{Hz}$ for V_{yy} and $12mE/\sqrt{Hz}$ for V_{zz}).

When estimating the gravity field parameters via a rigorous least-squares adjustment, this correlation pattern would normally have to be taken into account by including the known (or an estimated approximation of the) data covariance matrix (as a metric) into the normal equations. However, due to the huge number of SGG data, this covariance matrix cannot be stored considering a memory requirement of more than 20 PetaByte. An effective solution to this problem consists in a full decorrelation ("whitening process") of the SGG data before the evaluation of the normal equations[4] . Such a decorrelation can be performed effectively through an application of digital filters to the SGG observations and the corresponding observation equations (cf. [13], [14], [19] and [9]).

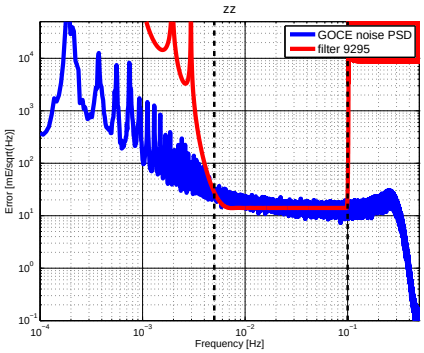

Figure 6. Noise PSD ans PSD for the inverse filter 9295 (MBW band-pass filter). The figure is only shown for th V_{zz} component. The other diagonal components have all very similar characteristics.

3. MODELING THE GRADIOMETER NOISE

After describing the main characteristics of the gradiometer noise in the previous section, we will focus on the modeling of the noise in the following subsections. As the full variance/covariance matrix of the gradiometer observations is even to large to be stored on supercomputers, the idea of describing the noise characteristics by an ARMA process was developed in [13]. The inverse process, which can be seen as a digital filter, can be used to decorrelate the observations and corresponding functional model. The transformed observation equations have white noise and are uncorrelated (e.g. [8], p. 154f.), such that the least squares adjustment in the gravity field determination can be performed with a covariance matrix equaling the identity matrix.

To get a better understanding of the coherence between digital filters and variance/covariance matrices, in [14] it is shown how a digital ARMA filter can be transformed to a variance/covariance matrix. To interpret the following figures of the noise and the estimated decorrelation filters in the spectral domain, remind that a filtering in the time domain is an element by element multiplication in the spectral domain. Thus, we need to find a filter with a spectral behavior inverse to the spectral noise behavior seen in Fig. 4. If we are able to find such a filter, the multiplication in the spectral domain would follow a curve constantly equaling 1.0, which is the PSD of white noise. Thus, we try to estimate a filter, which inverse PSD approximates the estimated PSD of the noise (cf. Fig. 4) as good as possible, under the additional condition that it can be described by as less as possible coefficients. Methods to estimate such filters of different complexity as cascades of ARMA filters are explained in detail in e.g. [14] and [19]. Within this contribution, we will not focus on the technical side, but show the influence of filters modeling the noise with different complexities.

[4]This means a complete decorrelation, as e.g. described in [8], p. 154f. of the observations and the functional model.

3.1. Concentrating on the measurement bandwidth

A first idea could be, to apply a filter, which focuses on the MBW, where the noise spectrum is flat and thus already close to white noise. Thus, a band-pass filter could be used to filter the signal and the functional model to the measurement bandwidth. An estimated (inverse) band-pass filter can be seen in Fig. 6, designed for the gradiometer's MBW, indicated by the black dashed lines. Applying this filter to the observation equations of the gradiometer measurements in the gravity field determination from gradiometer only observations, all information below the MBW is omitted (long wavelength noise but also parts of the signal). Thus, the high quality data within the MBW are processed, but the information outside the MBW is ignored in the estimation process.

Gravity field determination with such a kind of filter is possible – but has some disadvantages, as shown in the following. A gradiometer only gravity field solution computed with this filter is shown in terms coefficient differences to the 7 years based GRACE only model *ITG-Grace2010s* (cf. [10]) to the maximal resolution of the GRACE field which is d/o 180. Fig. 5(a) shows that the coefficient errors (i.e. coefficient differences to the GRACE model) to d/o 50 are very large. Note that to d/o 120 the GRACE model can be seen as a kind of reference solution, as GRACE is more sensitive to the lower degrees then the GOCE solution. The error per degree decreases from d/o 50 to d/o 100 but is still very large to d/o 100 for the sectorial coefficients[5].

These quality characteristics of the sectorial and near sectorial coefficients are reflected by the estimated spherical harmonic coefficient accuracies shown in Fig. 5(b). The standard deviations show, that the sectorial coefficients to degree 100 are bad determined as indicated in the coefficient differences to the *ITG-Grace2010s* model. The co-

[5]It should be mentioned in this context that intentionally a very moderate band-pass filter was chosen, where the noise reduction in the stop-band is only in the magnitude of 60 dB this avoids a singularity of the SGG gravity field solution.

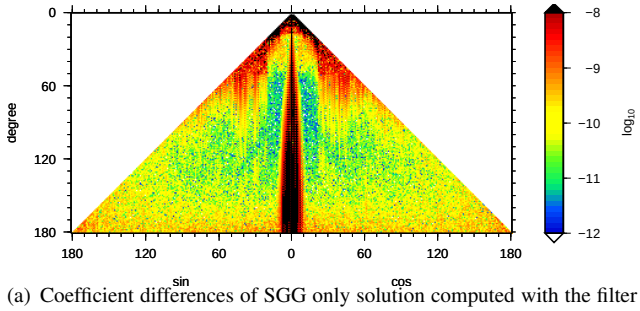

(a) Coefficient differences of SGG only solution computed with the filter 9295 compared to *ITG-Grace2010s*.

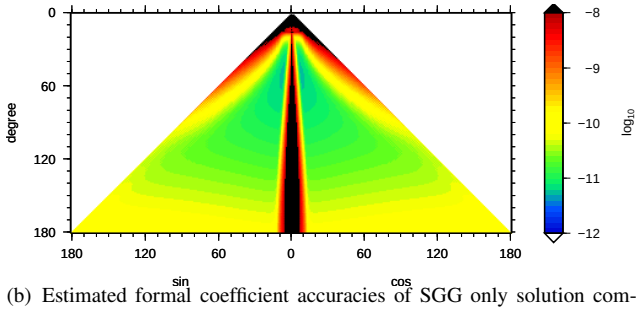

(b) Estimated formal coefficient accuracies of SGG only solution computed with the filter 9295.

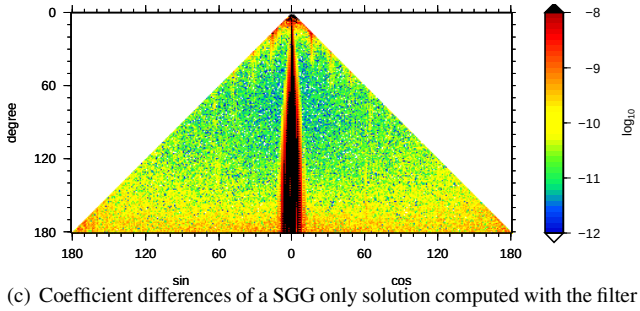

(c) Coefficient differences of a SGG only solution computed with the filter 1000 compared to *ITG-Grace2010s*.

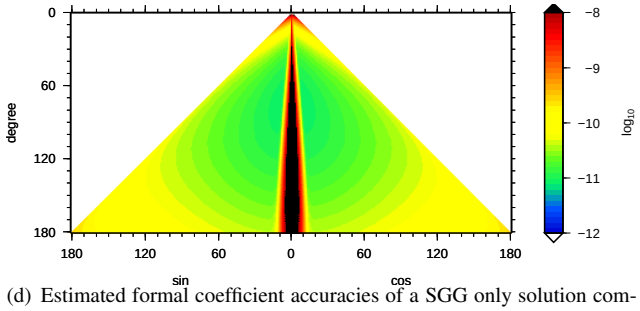

(d) Estimated formal coefficient accuracies of a SGG only solution computed with the filter 1000.

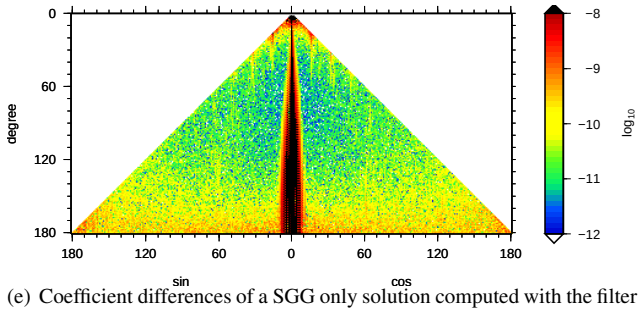

(e) Coefficient differences of a SGG only solution computed with the filter 9024 compared to *ITG-Grace2010s*.

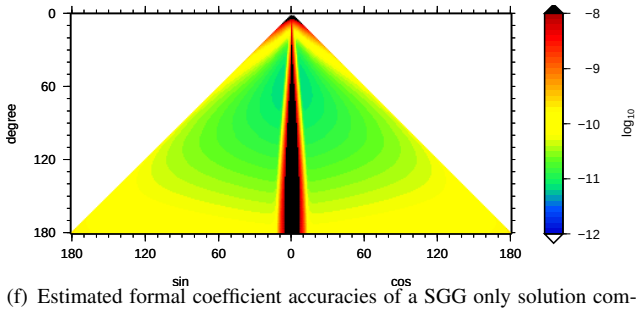

(f) Estimated formal coefficient accuracies of a SGG only solution computed with the filter 9024.

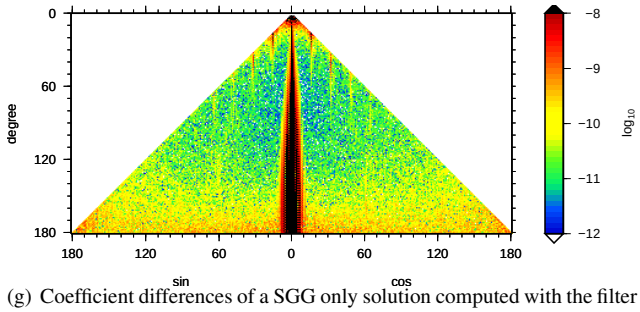

(g) Coefficient differences of a SGG only solution computed with the filter 9025 compared to *ITG-Grace2010s*.

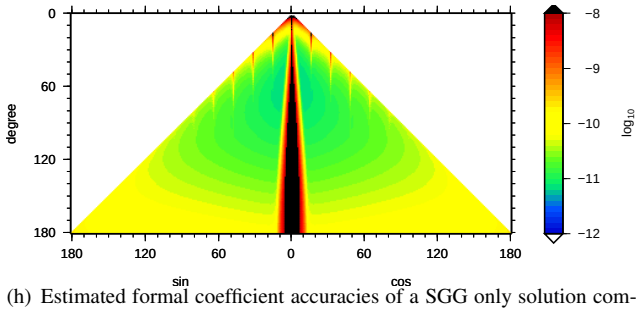

(h) Estimated formal coefficient accuracies of a SGG only solution computed with the filter 9025.

Figure 5. Coefficient statistics for all four presented SGG solutions with the four different filters. The shown statistics are difference to the ITG-Grace2010s *model (left column), estimated formal coefficient standard deviations (right column).*

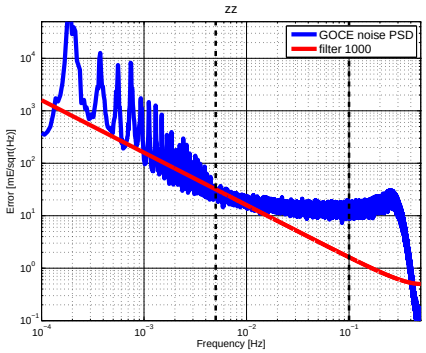

Figure 7. Noise PSD ans PSD for the inverse filter 1000 (differentiation filter). The figure is only shown for th V_{zz} component. The other components have all very similar characteristics.

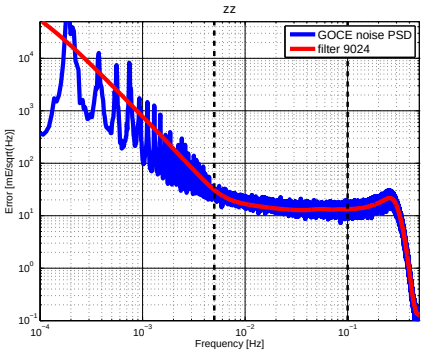

Figure 8. Noise PSD ans PSD for the inverse filter 9024. The figure is only shown for th V_{zz} component. The other components have all very similar characteristics

efficient differences compared to *ITG-Grace2010s* in the lower degrees show an agreement to the estimated variances. In the degrees 80 to 150, the differences to the GRACE model are well described by the corresponding GOCE accuracies. The displayed high degrees are dominated by the GRACE error, the GOCE variances show that GOCE performs better starting from degree 150. The high degrees 180-220, are not shown, as they cannot be compared to the lower degree GRACE model.

Using a band-pass filter as shown in Fig. 6 produces a useful gradiometer only gravity field and realistic estimates for the coefficient variances, but has the disadvantage that gradiometer information in the lower frequencies is ignored and that effects the sectorial coefficients to degree 100[6]. This can be more or less compensated when combining the gradiometer observation with the GPS observations from GPS tracking (SST).

3.2. Modeling the long wavelength errors

As the band-pass filter produces systematic errors for the sectorial coefficients, a further idea of the filter design would be to model the noise characteristics for the low frequencies. Thus a filter could be estimated, which down-weights the lower frequencies but keeps all information starting from the MBW. This means, we do not filter out the long wavelengths completely, but model their the poor quality in the adjustment. A very simple filter could be a differentiation filter (ID 1000) as shown in Fig. 7. These filter can be used to decorrelate the observed gradients and start the gravity field determination as a spherical harmonic series.

A comparison of a solution using this filter as stochastic information for the gradients to GRACE is shown in Fig. 5(c). Obviously the lower degree coefficient differences to GRACE (to d/o 80) are smaller than for the band-pass filter solution. The sectorial coefficients are determined well starting from d/o 20. It can be seen clearly in the variances, that the information outside the MBW contains information especially for the sectorial coefficients. The estimated accuracies in Fig. 5(d) show the better stability of the sectorial coefficients. The quality of the solution gets better, but the estimated accuracies have a wrong shape for the higher degrees (d/o 120+). The formal errors for the low orders of higher degrees are estimated too optimistic. This results from the incomplete modeling of the filter of the MBW frequencies. The filter introduces a weighting in the MBW which is not correct. Using the information of the whole spectrum seems to be a good idea, but a kind of mixture between the band-pass filter model and this filter model needs to be found to combine the advantages of both models.

[6]Note that the better the band-pass filter approximates an ideal band-pass filter the higher the degrees where the sectorial coefficients are estimated bad. The effect of ill-defined sectorial coefficients would be intensified with a higher noise reduction in the stop-band.

3.3. Simple modeling of the complete spectrum

Combining simple filters to a consecutive filter series (so call filter cascades) allow for the design of more complex filters. A filter should be designed which approximates the complete noise spectrum and not only parts of it, as did by the models before. Thus, in Fig. 8 a filter was designed modeling long wavelength errors as well as the MBW as good as possible. The smallest number of filter coefficients possible was used to keep the model simple.

The filter constitutes two cascades, one modeling the long wavelength part (similar to filter 1000) and a second one, an ARMA filter of a higher order modeling the high pass filtered rest correlations in the context of a least squares fit. Connecting both filter parts, the PSD plot in Fig. 8 shows the approximation of the noise. This filter with ID 9024 needs only 50 AR and 50 MA coefficients per gradiometer component to describe the whole noise behavior. Additionally it has only a short warmup (2000 positions will be lost as filter initialization). The resulting gravity field solution combines the advantages of the band-pass filter solution and the difference filter solution. The solution is at least as good as the difference

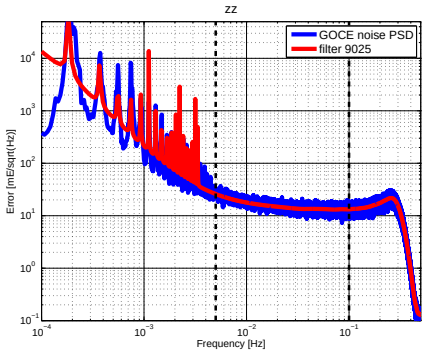

Figure 9. Noise PSD ans PSD for the inverse filter 1000. The figure is only shown for th V_{zz} component. The other components have all very similar characteristics

filter solution in all degrees (cf, Fig. 5(e)) as it shows mainly the same difference pattern compared to *ITG-Grace2010s*. The benefit of this modeling is visible in the estimated spherical harmonic coefficient standard deviations. The higher degree error is modeled very well by the estimated formal spherical harmonic coefficient errors (cf. Fig. 5(f)), the shape of the errors shows a good agreement for the errors compared to GRACE up to degree 150.

3.4. Complex modeling of the complete spectrum

Analyzing the filter with the ID 9024 (cf. Fig. 8), it can be seen that the n per revolution peaks in the spectrum are not modeled individually. Instead, this pattern is approximated simple (it seems to be linear in the double logarithmic plot). To improve the filter modeling, additional cascades could be added constituting special Notch filters (e.g. [19]) eliminating special frequencies from the signal. Thus, the filter is extended by several new filter cascades, each eliminating one of the sharp peaks in the spectrum. This filter (ID 9025) can be seen in Fig. 9. It consists of 20 cascades with about 100 AR and 100 MA coefficients. The notch filter cascades, realized as ARMA(2,2) filters, are responsible for a filter warmup of 200000 positions[7]. Computing a gradiometer-only gravity field solution with this kind of filter, we see no improvement in the solution (cf. Fig 5(g)) compared to the former model, but an improvement in the estimated variances is evident.

Comparing the coefficients estimated with filter 9024 and 9025 to the *ITG-Grace2010s* model coefficients, larger errors can be seen in the lower degree coefficients with the orders 16, 32, 48, 64. These are ill-defined coefficients due to the n per revolution error. Modeling these error peaks within the complex filter, these bad determined coefficients are indicated in the estimated coefficient accuracies (cf. Fig 5(h)). Thus, modeling the filter as complex as possible, we map the error structure

[7]This means, using this filter in the gravity field determination, 200000 observations are thrown away during the filter initialization.

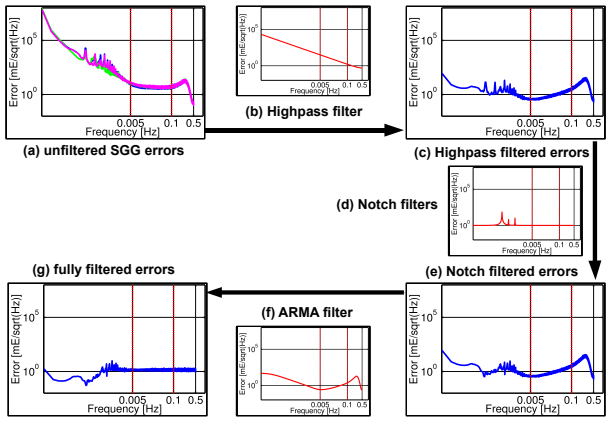

Figure 10. Effect of the different filter cascades in the decorrelation process illustrated in the spectral domain

of the GOCE gradiometer as good as possible to the coefficient accuracies of the estimated spherical harmonic expansion. Thus, we achieve a high quality and realistic formal error variance/covariance matrix. The effect of all cascades of this complex filter is summarized within Fig. 10.

4. COMBINATION WITH GPS OBSERVATIONS

Within SPF6000 the Tuning-machine is used to estimate a decorrelation filter for the gradiometer observation for the gravity field determination using the time wise approach amongst others. As the first GOCE gravity field model is only based on 71 days of gradiometer observations, we decided to use the simple filter 9024 for the final GO_CONS_EGM_TIM_2I solution. The simple filter model was preferred in order to keep the filter warmup short within the first short data period (2000 instead of 200000). But these complex filters will be used in future gravity field solutions, when the data period is longer and thus the coverage is better. It was shown above, that the filters are globally similar, but filter 9024 does not map the ill-defined orders to the variance/covariance matrix. At first, this seems to be uncritical, as this ill-defined orders are mainly in the low degrees, which are determined mainly by the GPS observations within the final solution. But, a look into the details shows that inconsistencies between the data and the covariance modeling stresses the combined solution. Modeling of the ill-defined orders in the gradiometer covariances yields to a higher weight of the GPS observations for this coefficients. This yields to a better final solution after combining gradiometer and GPS observations as the relative weights are more realistic.

Fig. 11 shows a combined GOCE solution, a gradiometer only solution (SGG) and a solution determined by GPS tracking (SST) using the energy balance approach (e.g. [3]). Fig. 11 shows an improvement of the combined so-

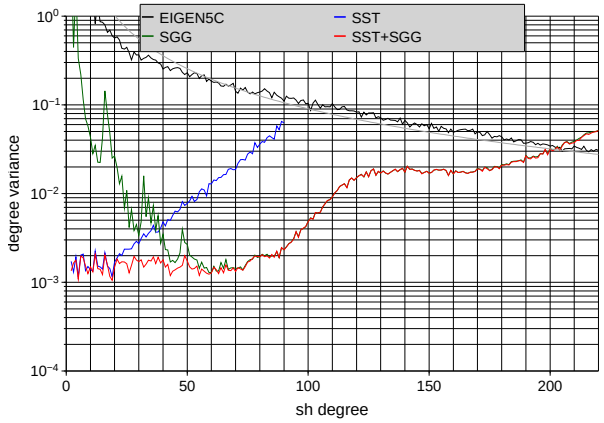

Figure 11. Degree variances estimated using coefficient differences to the EIGEN5C *model computed without the near zonal coefficients to exclude the effect of the polar gap. Shown is a gradiometer only solution (SGG), a solution only computed from the GPS tracking (SST) and the combined one, compared to the Signal of the* EIGEN5C.

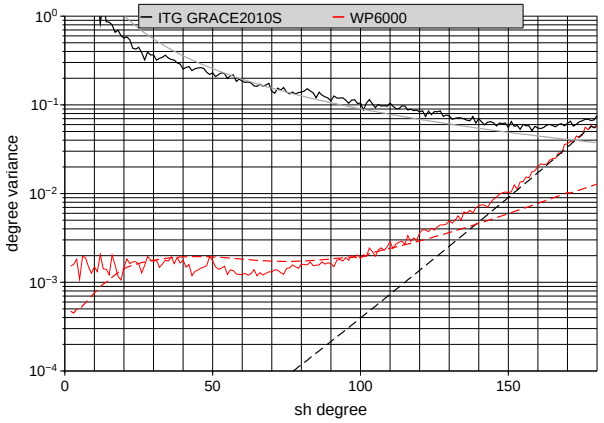

Figure 12. Degree variances estimated using coefficient differences to the ITG-Grace2010s *model computed without the near zonal coefficients to exclude the effect of the polar gap. Shown is the combined final WP6000 (GO_CONS_EGM_TIM_2I) solution compared to the GRACE only model* ITG-Grace2010s. *The degree variances estimated from formal errors are shown as a dashed line.*

lution from d/o 20 combining the SST only model with the SGG observations. This shows, that a long wavelength error modeling of the gradiometer noise is essential, if the best solution based on only GOCE observations should be determined.

Comparing the final GO_CONS_EGM_TIM_2I model to independently determined gravity field models, the consistence of the models in terms of degree variances can be shown clearly. Fig. 12 shows the final SPF6000 solution compared to the *ITG-Grace2010s* solution. Especially in the lower degrees, the 7 year based GRACE model is better than the GOCE only model based on just 71 days. The degree variances estimated from coefficient differences show a very good agreement with the estimated GOCE model accuracies to d/o 120. Starting from d/o 120 the GOCE solution becomes more accurate than the GRACE solution. For the very high degrees 150 - 180, where GOCE performs better, the GRACE accuracies show a good agreement to the difference to the GOCE model.

Fig. 13 shows the final GO_CONS_EGM_TIM_2I solution compared to the *EIGEN5C* model (c.f. [6]), which is a high degree combination model, including e.g. GRACE, altimetry and terrestrial data. For the low degrees (90) the combined model performs better than GOCE, due to the included GRACE observations. The estimated GOCE accuracies show again a consistent compared to the error estimated from the coefficient differences. From degree 90 to 190, GOCE improves the combined model, the accuracies of the combined *EIGEN5C* model follow the difference curve, as the GOCE accuracies are smaller. For the higher degrees 200+, the combined model performs better again, due to the high frequency sensitive terrestrial data included in the combination model.

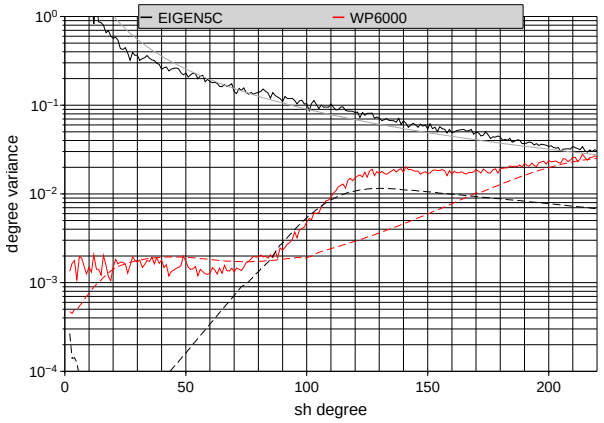

Figure 13. Degree variances estimated using coefficient differences to the EIGEN5C *model computed without the near zonal coefficients to exclude the effect of the polar gap. Shown is the combined final WP6000 (GO_CONS_EGM_TIM_2I) solution compared to the model* EIGEN5C. *The degree variances estimated from formal errors are shown as a dashed line.*

5. SUMMARY AND CONCLUSIONS

The presented tuned decorrelation filters are used within GOCE HPF SPF6000, determining a GOCE only gravity field using the so-called time-wise approach. We showed that we spent a huge numerical effort to determine digital filters, that can be used to decorrelate the GOCE gradient observations for the purpose of gravity field determination. We showed that a modeling of the complete error spectrum is essential to compute the best possible gravity field from GOCE observations. In addition, the full variance/covariance matrix will be distributed with the final solution (cf. [12]). Compared to independent

models (*ITG-Grace2010s* and *EIGEN5C*) the estimated formal accuracies show a consistent model. The provided variance/covariance matrix is of a very high quality, as it is modeled straight forward throughout all computation steps of GOCE only gravity field determination steps. As no external information is included in the solution, the solution and the variance/covariance matrix are thus self-consistent. We recommend to use the full variance/covariance matrix in as many applications as possible, where the GOCE model is used. As can be seen in comparison to independent models, the provided covariance matrix reflects the true error characteristics of the GOCE gravity field solution. With the coefficients and the full variance/covariance matrix, indirectly the full set of normal equations are available, which allows for the use in combination models (e.g. with GRACE, altimetry or terrestrial data).

ACKNOWLEDGMENTS

Parts of this work were financially supported by the BMBF Geotechnologien program REAL-GOCE and the ESA GOCE HPF contract No. 18308/04/NL/MM. The computations were performed on the JUROPA supercomputer in Jülich. The computing time was granted by John von Neumann Institute for Computing (project HBN15).

REFERENCES

[1] H. Alkhatib. *On Monte Carlo methods with applications to the current satellite gravity missions*. PhD thesis, Institute of Geodesy and Geoinformation, University of Bonn, Bonn, 2007.

[2] H. Alkhatib and W.-D. Schuh. Integration of the Monte Carlo covariance estimation strategy into tailored solution procedures for large-scaled least squares problems. *Journal of Geodesy*, 70:53–66, 2007.

[3] T. Badura. Gravity Field Analysis from Satellite Orbit Information applying the Energy Integral Approach. PhD thesis, TU Graz, Graz, 2006.

[4] C. Boxhammer. Effiziente numerische Verfahren zur sphärischen harmonischen Analyse von Satellitendaten. PhD thesis, Institute of Geodesy and Geoinformation, University of Bonn, Bonn, 2006.

[5] J.M. Brockmann, B. Kargoll, I. Krasbutter, W.-D. Schuh, and M. Wermuth. GOCE data analysis: From calibrated measurements to the global earth gravity field. In N.N., editor, *Observation of the Earth System from Space*, accepted. Springer, 2009.

[6] C. Foerste, F. Flechtner, R. Schmidt, R. Stubenvoll, M. Rothacher, J. Kusche, K.-H. Neumayer, R. Biancale, J.-M. Lemoine, F. Barthelmes, S. Bruinsma, R. Koenig, and U. Meyer. EIGEN-GL05C - A new global combined high-resolution GRACE-based gravity field model of the GFZ-GRGS cooperation. In *Geophysical Research Abstracts*, volume 10 of *General Assembly European Geosciences Union*, Vienna, 2008.

[7] M. Hestenes and E. Stiefel. Methods of conjugate gradients for solving linear systems. *Journal of Research of the National Bureau of Standards*, 49 (6), Research Paper 2379, 1952.

[8] K.R. Koch. Parameter Estimation and Hypothesis Testing in Linear Models. Springer Berlin/Heidelberg, 2 edition, 1999.

[9] I. Krasbutter. Dekorrelation und Daten-TÜV der GOCE-Residuen. Diploma thesis, Universität Bonn, Bonn, 2009.

[10] T Mayer-Gürr, E. Kurtenbach, and A. Eicker. ITG-Grace2010s. http://www.igg.uni-bonn.de/apmg/index.php?id=itg-grace2010, 2010.

[11] R. Pail, B. Metzler, B. Lackner, T. Preimesberger, E. Hck, W.-D. Schuh, H. Alkathib, C. Boxhammer, C. Siemes, and M. Wermuth. GOCE gravity field analysis in the framework of HPF: operational software system and simulation results. In 3^{rd} *GOCE user workshop*, Frascati, 2006. ESA.

[12] R. Pail, H. Goiginger, R. Mayrhofer, W.-D. Schuh, J. M. Brockmann, I. Krasbutter, E. Hck, and T. Fecher. GOCE gracity field model derived from orbit and gradiometry data applying the time-wise method. In *Proceedings of the ESA Living Planet Symposium*, Bergen, 28 June 2 July 2010. ESA.

[13] W.D. Schuh. SST/SGG tailored numerical solution strategies. Technical report, ESA-Project CIGAR III / Phase 2, WP 221, Final-Report, Part 2, 1995.

[14] W.-D. Schuh. Tailored Numerical Solution Strategies for the Global Determination of the Earth's Gravity Field, volume 81 of *Mitteilungen der geodätischen Institute der Technischen Universität Graz*. TU Graz, Graz, 1996.

[15] W.-D. Schuh. The processing of band-limited measurements; filtering techniques in the least squares context and in the presence of data gaps. In G. Beutler, M.R. Drinkwater, R. Rummel, and R. von Steiger, editors, *Earth Gravity Field from Space - From Sensors to Earth Sciences*, volume 108, pages 67–78. Space Science Reviews, 2003. ISSI Workshop, Bern (March 11-15,2002).

[16] W.-D. Schuh, C. Boxhammer, and C. Siemes. Correlations, variances, covariances — from GOCE signals to GOCE products. In 3^{rd} *GOCE user workshop*, Frascati, 2006. ESA.

[17] W.-D. Schuh, J.M. Brockmann, B. Kargoll, and I. Krasbutter. Adaptive Optimization of GOCE Gravity Field Modeling. In G. Münster et. al., eds, *NIC Symposium 2010*, *IAS Series*, 3:313–320, Jülich, 2010.

[18] H.R. Schwarz. Die Methode der konjugierten Gradienten in der Ausgleichsrechnung. *ZfV*, 95:130–140, 1970.

[19] C. Siemes. Digital Filtering Algorithms for Decorrelation within Large Least Squares Problems. PhD thesis, Institute of Geodesy and Geoinformation, University of Bonn, Bonn, 2008.